Iterated Filter Banks with Rational Rate Changes Connection with Discrete Wavelet Transforms

Thierry Blu

Abstract—**Some properties of two-band filter banks with rational rate changes ("rational filter banks") are first reviewed. Focusing then on iterated rational filter banks, compactly supported limit functions are obtained, in the same manner as previously done for dyadic schemes, allowing a characterization of such filter banks. These functions are carefully studied and the properties they share with the dyadic case are highlighted. They are experimentally observed to verify a "shift property" (strictly verified in the dyadic case) up to an error which can be made arbitrarily small when their regularity increases. In this case, the high-pass outputs of an iterated filter bank can be very close to samples of a discrete wavelet transform with the same rational dilation factor. Straightforward extension of the formalism of multiresolution analysis is also made. Finally, it is shown that if one is ready to put up with the loss of the shift property, rational iterated filter banks can be used in the same manner as if they were dyadic filter banks, with the advantage that rational dilation factors can be chosen closer to 1.**

I. Introduction

FILTER banks have been in use in signal processing (mostly for coding purposes) since the mid-1970's using the property that "quadrature mirror filters (QMF)" [6] achieved aliasing cancelation. On the other hand, the mid-1980's saw the wide development of *constant-Q* analysis [9], [12] in the field of the analysis of nonstationary processes, in conjunction with studies on wavelet transforms. Finally, both fields were unified when it was shown [16] that the outputs of a two-band iterated dyadic filter bank (the bank is built from halfband filters subsampled by 2; iterated on the lowpass one) are samples of a continuous wavelet transform. The *multiresolution analysis* [16], [18] gave an entirely new perspective on the tree structure of iterated filter banks, by associating the reconstruction procedure to a dual biorthogonal multiresolution analysis [4]. Essentially, the breakthrough in the wavelet domain brought new ideas into the filter bank domain. The communication between both fields led, for example, to the design of fast wavelet transform using the simple structure of iterated filter banks [10], [21], [24]; as a converse influence, the regularity of the associated wavelets became a potentially important property for filter design. This last point has been deeply investigated from the mathematical point of view [7], [8], [20].

It seems that in spite of the advantage of developing any function into an orthonormal wavelet series, the iterated filter bank schemes were used for analysis purposes only through the fast algorithm for the computation of the wavelet transform. A reason for this is that they imply octave-band decomposition, which is often much too coarse for analyzing signals such as high quality audio or speech. This has a number of consequences: for using the fast algorithm based on the two-band iterated filter bank, it is necessary to design as many filters as the number of "voices" which is required per octave (an octave is decomposed into subbands, which are named "voices" in [21]).

Another, more direct way to solve this problem would be to use rational iterated filter banks (Fig. 1); here the signal is separated in a much more dense set of frequency bands. At first sight, one could reasonably hope that this scheme provides a wavelet analysis of the input signal, like in the dyadic case. In more detail, it appears that strictly speaking, this is not the case. It is still possible to define a kind of multiresolution analysis, but this one is no longer built from dilated and shifted versions of a single function φ; instead, an infinite set of dilated "almost"-shifted bricks (in a sense which will be defined laser) are used to build this rational multiresolution analysis. In the dyadic case, these functions $\varphi_n(t)$, are shifted versions $\varphi(t - n)$, a connection which does not hold in the rational FIR case (in the IIR case, see [1], [14]).

This paper works out these discrete rational architectures in order to precisely characterize the associated analog time-frequency analysis, its properties, and focus on its differences with the wavelet analysis. It will also be illustrated that the difference between the more general rational multiresolution analysis and the classical dyadic one can be made as small as desired by enforcing some regularity constraints to the basic filters. However, the paper only intends to give an introduction to these new functions. In particular, short or accessible proofs will be given, but due to the lack of space, not every question will be tackled, even if the dyadic case shows how to answer them.

Previous work on the general rational filter bank architectures can be found in [2], [5], [11], [14], [19], [26]. Among these, the work of Kovačević and Vetterli [14]

Manuscript received July 1, 1992; revised May 13, 1993. The Guest Editor coordinating the review of this paper and approving it for publication was Dr. Ahmed Tewfik.

The author is with France Telecom-CNET, 38-40 rue du General Leclerc, 92131 Issy-les-Moulineaux, France.

IEEE Log Number 9212172.

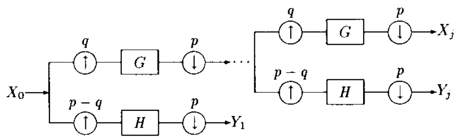

Fig. 1. Iterated analysis rational filter bank.

has most deeply influenced us. In particular, they gave a method for designing perfect reconstruction rational filter banks, and were the first to think about iterating it, as it is often done in the dyadic case.

Various methods are available in order to find the synthesis FIR filter bank allowing the perfect reconstruction of a signal processed by an analysis two-band rational filter bank. There are either analytical [11], [26], or numerical methods [19]. We use the one in [11] and write down in Section II, the corresponding equation in the same polynomial matrix form as can be done in the dyadic case; this equation is later used in Section V. Section III discusses the iteration of such rational filter banks, providing the basic tools that are used later on. In the same section, the associated arithmetic complexity of such a tree structure is given. Section IV deals with the main subject of the paper, which is the existence of basis functions characterizing the generalized multiresolution analysis. They are obtained through a limit process, and shown to obey a generalized two-scale difference equation; this equation is indeed very similar to the one studied by Daubechies and Lagarias [8] in the dyadic case. The properties of these limit functions allow unsolved questions stated by Kovačević and Vetterli in their work on iterated rational filter banks to be explained. The fact that Cohen and Daubechies [3] proved that a multiresolution analysis cannot be built with rational dilation factors together with FIR low-pass filters, may explain why the former authors finally admitted that the iteration of a synthesis filter bank cannot generate a limit function. Actually, several different limit functions are obtained, depending in a complex manner on the chosen initialization. This is the only important difference with the dyadic case. This difference is due to the absence of a shift property, which can however be made very small by an appropriate choice of regular filters.

Section V shows that a rational scheme is equivalent to some continuous wavelet-like analysis, which is explicitly stated. Moreover, we illustrate that all the properties of the dyadic architecture (wavelet transform and wavelet series) have a straightforward equivalent in the rational case. It is hoped that since the shift error can be made as small as possible, the simpler expressions of the dyadic case will be reasonable approximations of the general rational case.

To be fair, we must emphasize that the gain in frequency resolution brought by the rational analysis might by some aspects be counterbalanced by a greater complexity, especially as far as filter design is concerned. The reduction of the shift error, for example, is linked to the regularity of the limit functions, and the need for a given order of differentiation requires longer filters in the rational case than in the dyadic one; typically, if a filter of degree at least N is needed in the dyadic case to achieve $N - 1$ bounded derivatives, a filter of degree at least $N(p-1)$ is required in the rational case for the same purpose.

Notations

We use the following notations throughout the paper.

- To a sequence $x[n]$ corresponds a series $X(z)$ (z-transform) defined by $X(z) = \Sigma_k x[k]z^{-k}$.
- The greatest integer less than or equal to x is denoted by $\lfloor x \rfloor$.
- The matrices are denoted $\boldsymbol{A} = [A_{k,l}]$ where k, l are the row and column index, respectively.

II. Rational Filter Banks

The *rational filter bank* is shown in its general form in Fig. 2. Here, the input signal X is analyzed by N branches each one of the form shown in Fig. 3; the rate of any output Y_i is a fraction q_i/p_i of the incoming rate. The assumptions of [14] are $\gcd(q_i, p_i) = 1$, since any possible common divisor can be canceled by an appropriate change of the filter, and $\Sigma_{i=0}^{N-1} q_i/p_i = 1$, so that the global output rate equals the input rate. This rate conservation lies between two cases. The first one $\Sigma_{i=0}^{N-1} q_i/p_i < 1$, for which perfect reconstruction cannot be reached since a certain amount of information is lost in the analysis process. The second one $\Sigma_{i=0}^{N-1} q_i/p_i > 1$ for which, in general, perfect reconstruction can be reached, but with several different synthesis processes, since now the analysis generates redundant outputs.

In order to undertake a "rational analysis" as explained in the Introduction, it is clear that each branch of the scheme has to perform a "rational interpolation" of a signal at time samples which are not integer divisors of the reference sampling rate. We show by an example (slightly adapted from [23]) that it is indeed the case for each branch of a rational filter bank. Assume that the bank-limited signal $x(t)$ can be perfectly reconstructed from its subsamples $x(n\tau)$ via Nyquist relation $x(t) = \Sigma_k x(k\tau)\chi(t/\tau - k)$ with $\chi(t) = \sin(\pi t)/(\pi t)$. Thus, changing the sampling rate from τ to $p\tau/q$ gives

$$x\left(\frac{p}{q} n\tau\right) = \sum_k x(k\tau)\chi\left(\frac{np - kq}{q}\right). \tag{1}$$

This equation simply states that the input sampled signal $x[n] = x(n\tau)$ is first up-sampled by q, then filtered by the low-pass filter $G(z) = \Sigma_k \chi(k/q)z^{-k}$, and finally down-sampled by p. This is the general form of the "branch operator" depicted in Fig. 3

$$y[n] = \sum_k g[np - kq]x[k]. \tag{2}$$

This paper now concentrates on the two-band rational filter bank, and on its iterations. We recall some properties of the basic cell, which are direct extensions from what was stated in previous literature [25], [27].

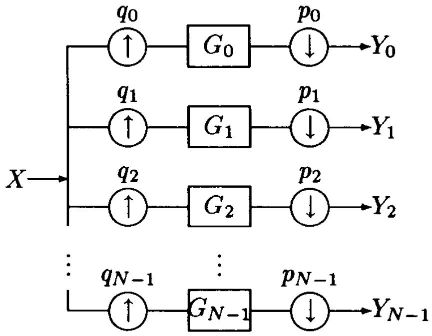

Fig. 2. N-band rational filter bank.

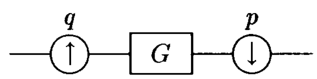

Fig. 3. The basic operator of rational filter banks.

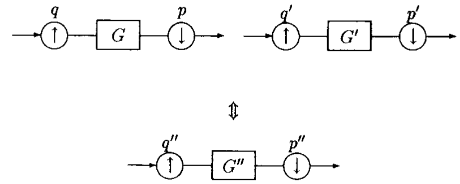

Fig. 4. Composition property.

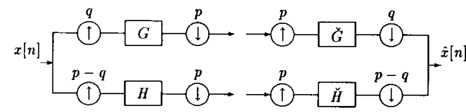

Fig. 5. Analysis–synthesis.

A. Composition Property

First note that the composition of two branches is in general still a branch of the same type, provided that the down-sampling factor of the first branch be prime with the up-sampling factor of the second one. This allows the construction of large rational filter banks by iterating a unique two-band rational filter bank as we shall proceed in Section III. Indeed, with the notations of Fig. 4, provided $\gcd(p, q') = 1$, the two branches can be contracted to one, with

$$p'' = pp' \tag{3}$$

$$q'' = qq' \tag{4}$$

$$G''(z) = G'(z^p)G(z^{q'}). \tag{5}$$

The proof is easily obtained in three steps, using basic properties of the composition of filters and up- or down-sampling operators [26].

- Since p and q' are coprime, they can be swapped.
- $G(z)$ followed by up-sampling by q' is equivalent to up-sampling by q', followed by filtering by $G(z^{q'})$.
- Filtering by $G'(z)$ preceded by down-sampling by p is equivalent to filtering by $G'(z^p)$ followed by down-sampling by p.

B. Inversion

We now address the question of reconstructing an input signal x_0, given its two outputs x_1 and y_1 through, respectively, the low-pass branch ($q \uparrow G \downarrow p$) and the high-pass one ($(p - q) \uparrow H \downarrow p$). It turns out that in the two-band case, the reconstruction structure is simply the mirror of the analysis structure, involving in general *different* filters $\check{G}$ and $\check{H}$ as shown in Fig. 5. The proof of this property stems from [13], [14] where it is shown how to transform an analysis rational filter bank as in Fig. 2 into a uniform filter bank; it can thus be inverted. In our simple two-band case where p is coprime with q and $p - q$, the composition of the inverse transformation [13], [14] with the inverse uniform filter bank results in a mirror structure of the analysis rational filter bank.

The reconstruction filters can thus be computed by a simple matrix inversion, as in the integer case. In [13], [14], the analysis matrix is obtained after the decomposition of the output signal into polyphase components . Here, we use an alternative method which amounts to the decomposition of the output as well as the input of a given branch into polyphase components [11], [26]. For every signed integer n, we define

$$G_n(z) = \sum_k g[n + kpq]z^{-k} \tag{6}$$

$$X_n(z) = \sum_k x[n + kp]z^{-k} \tag{7}$$

$$Y_n(z) = \sum_k y[n + kq]z^{-k} \tag{8}$$

as, respectively, the pq, p, and q polyphase components of $G(z)$, $X(z)$, and $Y(z)$. This is a definition of the polyphase components which is slightly different than usual, since n is not limited to $[0 \cdots pq - 1]$, $[0 \cdots p - 1]$, and $[0 \cdots q - 1]$, respectively. However, it allows the derivation of simpler formulas by eliminating the need for the function "integer part" or "modulo." In terms of the polyphase components, the low-pass branch (2) reads

$$y_{n_0}[n_1] = \sum_{k_0=0}^{p-1} \sum_{k_1} g_{n_0 p - k_0 q}[n_1 - k_1]x_{k_0}[k_1] \quad \text{for } n_0 \text{ between 0 and } q - 1 \tag{9}$$

and, in terms of z-transforms

$$Y_{n_0}(z) = \sum_{k_0=0}^{p-1} G_{n_0 p - k_0 q}(z)X_{k_0}(z) \quad \text{for } n_0 \text{ between 0 and } q - 1. \tag{10}$$

This equation provides the q polyphase components of $Y(z)$ as a sum of filtered versions of the p polyphase components of the input $X(z)$. It can be written in matrix form. The transfer matrix is built from the pq polyphase components of G. Interverting p and q in (2) provides a similar formula for a synthesis branch. For the high-pass branch,

q is changed to $p - q$, and we define

$$H_n(z) = \sum_k h[n + kp(p - q)]z^{-k} \tag{11}$$

as the $p(p - q)$ polyphase component of $H(z)$.

With this notation, the global analysis–synthesis operation reduces to a product of two matrices. In case of a (noncausal) perfect reconstruction system this product should be identity

$$\underbrace{([\check{G}_{kq-lp}]\ [\check{H}_{k(p-q)-lp}])}_{\check{\Gamma}} \underbrace{\begin{pmatrix} [G_{kp-lq}] \\ [H_{kp-l(p-q)}] \end{pmatrix}}_{\Gamma} = Id \tag{12}$$

where the first two submatrices (from the left) are rectangular of respective dimensions $p \times q$ and $p \times (p - q)$, and the other two have corresponding transpose dimensions. Each matrix Γ is thus of dimension $p \times p$. Finally, one can say that perfect FIR reconstruction requires the same condition as in the integer case, that is to say $\det(\Gamma) = Cz^n$; if this is not true, IIR synthesis filters are necessary.

III. Iterated Rational Filter Banks

We now consider the iteration on the low-pass filter $G(z)$ of a 2-band rational filter bank such as the one in Fig. 1, as is usual in the dyadic case. After the jth iteration, the architecture is equivalent to a $(j + 1)$-band rational filter bank as in Fig. 2, which is efficiently computed via this tree structure. The relative simplicity of a two-band filter band leads to simple understanding of that particular $(j + 1)$-band filter bank. Moreover, iterating on the sole low-pass filter involves an approximate "constant-Q" decomposition, which will be shown in Section V to be similar to a wavelet decomposition [16], [17] with p/q as scale factor.

A. Iteration

After j iterations, the global operation remains linear and, using the composition relation, we find that

$$x_j[n] = \sum_k g_j[np^j - kq^j]x_0[k] \tag{13}$$

where the involved filters G_j are defined by recurrences on their z-transform

$$G_{i+j}(z) = G_i(z^{p^j})G_j(z^{q^i}) \tag{14}$$

$$G_j(z) = G(z^{p^{j-1}})G(z^{qp^{j-2}}) \cdots G(z^{q^{j-1}}) \tag{15}$$

for j greater than or equal to 1, G_0 being equal to 1. These formulas are simple and are immediate extensions of the dyadic case. But there is one qualitative feature that is important for what follows; when $q = 1$, a delay of 1 at stage j means a delay of p^j for the input signal but, if $q \neq 1$ it would correspond to a delay of $(p/q)^j$ for x_0. This would not be a problem with a perfect interpolation, in which case the outputs could easily be considered as samples of a wavelet transform. However, the actual interpolation, being made from finite length FIR filters, is not perfect, and involves different filters depending on the precise phase of the interpolated sample. Since a shift of q^j for the output corresponds to a shift of p^j for the input, this tends to indicate that q^j wavelets have to be introduced. This intuition will be confirmed in Section IV-F where we show that after iteration j, q^j different estimates for the limit functions are generated. This explains why the outputs of a rational filter bank cannot generally be seen as sampled versions of a discrete wavelet transform. Notice that this problem does not arise in the dyadic case where $q = 1$.

B. Complexity

The advantage of critically sampled iterated filter banks is that the throughput at the output of the bank is the same one as the input sampling rate. Letting the low- and high-pass filters G, H be of length L and l, respectively, the output of the low-pass branch has a throughput equal to q/p, while the output of the high-pass branch has a throughput equal to $(p - q)/p$. The number of multiplications plus additions is approximately L/p and l/p for the low- and the high-pass, respectively. If we sufficiently iterate the two-band scheme, we get

$$\frac{L + l}{p - q} \text{ mults + adds per input sample.} \tag{16}$$

At first sight, there is no change between the dyadic case ($p = 2$, $q = 1$) and the rational case where $p - q = 1$. It could even seem more interesting, if one tries to mimick an octave band decomposition by a rational scheme, to use $p = 2q - 1$ (whence $p/q \approx 2$) which leads to a division by almost q of the complexity, as compared to the dyadic case!

In fact, L implicitly depends on q and l on $p - q$ since the filters are designed in the up-sampled domain. These lengths must be multiplied by q and $p - q$ (respectively) in order to retain the same performance in terms of filter design as in the dyadic case; this breaks the paradox evoked above. As a consequence, the rational case is in general much more difficult to design since longer low-pass filters are required to meet the same selectivity (width of the transition band, attenuation) as in the dyadic case. Whenever $p - q = 1$, an effect of the finer frequency resolution is the increase of the complexity approximately by a factor q over the dyadic case.

IV. Limit Functions

The connection between iterated filter banks and discrete wavelet transforms has constituted a strong catalyst in both fields of nonstationary sampled signals analysis and mathematical analysis. In particular, it pointed out the importance of the time behavior of the functions which can be generated by the infinite iteration of a synthesis low-pass branch. By construction, these functions verify what was to be named a *two-scale difference equation* [8]. Although they were supposed to be interpolating functions, they could behave in a pathological way; for example, they could be continuous but not differentiable "almost everywhere." This problem called for accurate regularity estimates obtained from the filter coefficients [8], [20].

This section follows the same path in the rational case as was taken in the dyadic one. More specifically, we are interested in the possible convergence of the impulse response of the iterated low-pass synthesis filter towards a function in the rational case. When this convergence occurs, we characterize as precisely as we can the properties of this limit such as its support, its smoothness, and others. Due to the peculiarity of the rational case, which have already been outlined (absence of shift property), this study requires the use of FIR filters in the general (noncausal form

$$G(z) = \sum_{k=M}^{L} g[k]z^{-k} \tag{17}$$

$$H(z) = \sum_{k=m}^{l} h[k]z^{-k}. \tag{18}$$

These filters will be indifferently analysis or synthesis filters, corresponding either to Fig. 7 or Fig. 8 (this will be clear from the context). This fuzziness is necessary, since we generate limit functions at the synthesis side of Fig. 8, using the notations of Fig. 6; these functions are used to interprete the analysis side of the situation in Fig. 7, using the notations of Fig. 1. We first briefly review the dyadic case [20].

A. Dyadic Case

Consider the synthesis side of Fig. 8 in the dyadic case $q = 1$ and $p = 2$. When the inputs of the high-pass filters are set to zero and the one of the low-pass filter is set to z^{-s}, the scheme simplifies to the iterations of Fig. 6. For $s = 0$, the output of the system is the impulse response $g_{j,0}[n] = g_j[n]$ of the jth iterated low-pass filter. Under certain conditions, we can define a function $\varphi(t)$ such that $g_j[n]$ approaches $\varphi(n/2^j)$ as j tends to infinity.

The general result is that the condition $G(1) = 2$ ensures the existence of a distribution φ such that for any compactly supported C^∞ function $f(t)$, $1/2^j \Sigma_k g_j[k]f(k/2^j)$ converges to $\int \varphi(t)f(t)\,dt$ when j tends to infinity. This function (or distribution) meets the following two-scale difference equation [8], [20]:

$$\varphi(t) = \sum_k g[k]\varphi(2t - k). \tag{19}$$

Several other properties are associated to this function.

- $\varphi(t)$ has bounded support $[M, L]$.
- If the input X_0 is delayed, say $X_0(z) = z^{-s}$ then the limit function is in fact the shifted function $\varphi(t - s)$ (shift property).
- Consider now the iteration on the analysis side of Fig. 7 or Fig. 1 with the same filter $G(z)$; $\varphi(t)$ still denotes the limit function generated by the same filter at the synthesis side of Fig. 8. Assume that the input $x_0[n]$ can be written as the nth sample of some analog function $x(t)$ weighted by the limit function $\varphi(t)$ under the form $\int x(t)\varphi(n - t)\,dt$. Then it has been shown [16] that the outputs of the analysis iterated filter bank of Fig. 7 are given by

Fig. 6. Iteration of the low-pass filter with $G_{0,s}(z) = z^{-s}$.

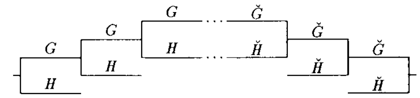

Fig. 7. Simplified iterated analysis–synthesis scheme.

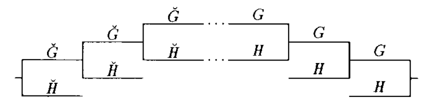

Fig. 8. Simplified iterated analysis–synthesis scheme, reversed structure of Fig. 7.

$$x_j[n] = \int x(t)\varphi(n - 2^{-j}t)\,dt \tag{20}$$

$$y_j[n] = \int x(t)\psi(n - 2^{-j}t)\,dt \tag{21}$$

where $\psi(t) = \Sigma_k h[k]\varphi(2t - k)$. In other words, the high-pass filter outputs are samples of a wavelet transform for scales $2^{-1}, 2^{-2}, \cdots, 2^{-j}$.

The latter property naturally states the question of the links between properties of "good" transforms [hence of "good" functions $\varphi(t)$], and properties of the low-pass filter $G(z)$. One of these desired properties is the regularity of the function, i.e., its continuity, derivability, and so on. It can be proven that pointwise convergence requires $G(1) = 2$ and $G(-1) = 0$, a condition which is not sufficient. More generally, $1/2^N(1 + z^{-1})^N G(z)$ generates a function which is N times more regular than the one associated to $G(z)$; that function is C^N if the latter is C^0 [20]. The next subsections discuss the extension of these properties to the rational case.

B. A Definition of Convergence

We want to give a meaning to the "convergence of $g_j[n]$ to $\varphi(t)$" when j tends to infinity. Two different definitions are useful for this purpose. We say that

- $g_j[n]$ converges weakly to $\varphi(t)$ if and only if, for all C^∞ function f with bounded support

$$\lim_{j\to\infty} \left(\frac{q}{p}\right)^j \sum_k g_j[k] f\left(k\left(\frac{q}{p}\right)^j\right) = \int \varphi(t)f(t)\,dt \tag{22}$$

- $g_j[n]$ converges pointwise (or strongly) to $\varphi(t)$ if and only if, there exists a constant C such that for all $\epsilon > 0$, there exists an integer J implying

$$\text{for all } j \geq J \text{ then } \begin{cases} |g_j[k] - \varphi(t)| \leq \epsilon \\ \text{where } |k - (p/q)^j t| \leq C. \end{cases} \quad (23)$$

Of course, the strong convergence implies the weak one. The first definition is a kind of convergence "in the sense of distributions" which needs not be pointwise, but rather emphasizes on the mean value of a limit.

An example in the dyadic case exemplifies the potential of this definition. Let $G(z) = (z^{-2} + 1)^2/2$, and consider the discrete sequence $x_j[n] = g_j[n]$. The low-pass filter $G(z)$ does not verify $G(-1) = 0$ and thus fails to generate a pointwise limit. In detail, since $G(z)$ is even $g_j[2n + 1] = 0$, while the even terms $g_j[2n]$ converge to a nontrivial function.

However, the generating polynomial is simply the dilated version by 2 of $(z^{-1} + 1)^2/2$, whose dyadic schemes converge pointwise to the B-spline of order 2 (piecewise linear). By using weak convergence instead of pointwise convergence, this trouble disappears, and both schemes converge. We can expect to face the same problems in the rational case.

Moreover, if we only concentrate on the analysis side, it has been outlined in the previous section [see (20), (21)] that the limit function and its shifted/dilated versions are involved as a kernel in the inner product with the input signal. This tends to show that the weak convergence is a more adequate way to characterize the iteration scheme, at least on the analysis side.

Whenever it is sufficient to prove our results, we thus assume only weak convergence. In some cases, however, we must resort to the stronger pointwise convergence. This is in particular the case for the biorthonormality relations (Section V).

C. A Two-Scale Equation

We now study the infinite iteration of rational schemes, and show that they generate limit functions as in the dyadic case. After describing the iteration process, we show that a simple normalization at $z = 1$ is not sufficient to ensure convergence, even in a weak sense, to a nontrivial function. An example of strong convergence will be however given in Section IV-E. When there is at least weak convergence, then these functions obey a two-scale equation, which differs from the dyadic one by the loss of the shift property.

1) Iteration: Once again, consider the low-pass iterations of the synthesis side of Fig. 8, which is now a purely rational filter bank scheme. Iterating this scheme with null inputs at the filters H corresponds to iterating j times the low-pass synthesis filter, with input $G_{0,s}(z) = z^{-s}$ (see Fig. 6). The corresponding outputs are sequences $g_{j,s}[n]$ where the delay s is a parameter. They obey the following equations, deduced from (13)–(15)

$$g_{j,s}[n] = g_j[nq^j - sp^j] \quad (24)$$

$$g_{j+1,s}[n] = \sum_k g[nq - kp]g_{j,s}[k] \quad (25)$$

$$= \sum_k g_{j,k}[n]g[kq - sp] \quad (26)$$

$$g_{i+j,s}[n] = \sum_k g_{i,k}[n]g_{j,s}[k]. \quad (27)$$

Let us choose $s = 0$ for a while, and wonder whether the sequence $g_{j,0}[n]$ converges either in the weak or the strong sense to a nontrivial low-pass function $\varphi_0(t)$. The answer is yes; but there are additional constraints to the simple normalization condition arising in the dyadic case. Remember that in that case, $G(1) = 2$ is enough to enforce weak convergence of the dyadic schemes, for any nonzero polynomial.

2) Nonconvergence Example: A simple example shows the difference between rational and dyadic schemes about convergence. Let us choose the low-pass filter to be a simple delay $G(z) = z^{-1}$.

- *Dyadic Case:* The iterations provide $G_j(z) = z^{-2^j+1}$. This leads, after multiplication of $G(z)$ by 2 for normalization, to the distribution $\delta(t - 1)$, under weak convergence.
- *Rational Case $p = 5$, $q = 3$:* The iterations provide $G_j(z) = z^{(3^j - 5^j)/2}$. Clearly $g_{j,0}[n] = 0$ everywhere but for the initial value $j = 0$. Thus, $g_{j,0}[n]$ does not converge to a nontrivial limit. Furthermore, even if we change the initialization by choosing another value for s, it is easily seen that, for large j, $g_{j,s}[n] = 0$ everywhere. This implies that for any s, whatever the normalization, the only possible limit function vanishes.

Unfortunately, we do not know which minimum necessary and sufficient condition on the polynomial would lead to a weak converging scheme. Instead, we provide necessary conditions for the scheme to converge in a strong sense. Using this necessary condition, we could always obtain converging schemes. This is the case for the generating polynomial $G(z) = (1 - z^{-p})/(1 - z^{-1})$, considered later in Section III-E.

3) Equation: Even if convergence is ensured, there is still a huge difference between the dyadic and rational cases: the shift property is lost. Depending on the initial delay s, the limit function $\varphi_s(t)$ is different from $\varphi_0(t - s)$. Assume that convergence to the limit functions is weak, then we show below that these functions satisfy a modified two-scale equation

$$\varphi_s(t) = \sum_k g[kq - sp]\varphi_k\left(\frac{p}{q}t\right). \quad (28)$$

Proof: Let $f(t)$ be a C^∞ compactly supported function. Thanks to (26), we can write

$$\sum_{s'}\left[\left(\frac{q}{p}\right)^j \sum_k g_{j,s'}[k] f\left(k\left(\frac{q}{p}\right)^j\right)\right] g[s'q - sp]$$
$$= \left(\frac{q}{p}\right)^j \sum_k g_{j+1,s}[k] f\left(k\left(\frac{q}{p}\right)^j\right). \quad (29)$$

Assuming the weak convergence of $g_{j,s}[n]$ to the set of functions $\varphi_s(t)$ and noting that the summation over s' is finite, we take the limit of both sides. This implies that

$$\int \sum_{s'} g[s'q - sp]\varphi_{s'}(t)f(t)\, dt = \frac{p}{q} \int \varphi_s(t) f\left(\frac{p}{q} t\right) dt \tag{30}$$

is true for any C^∞ compactly supported function f. This means that (28) is true in the sense of distributions. □

In the $p = 2$, $q = 1$ case, and adding the restrictive constraint of the shift property $\varphi_s(t) = \varphi_0(t - s)$, this equation reduces to the classical dyadic two-scale difference equation [8]. The more general formulation in the rational case induces new properties. In fact, given a particular set of solutions verifying (28), we can construct other sets $f_s(t)$ with the help of any distribution $\lambda(t)$ by the formula

$$f_s(t) = \int \lambda(a)\varphi_s(at)\, da. \tag{31}$$

As an example, if the functions $\varphi_s(t)$ are solutions of the equation, so are the functions $t\varphi_s'(t)$, and so are the functions $t^2\varphi_s''(t)$, and so on . . . all these functions having the same supports. In the dyadic case, it was possible to study the function φ directly from its two-scale difference equation, or from its Fourier equivalent. But in the rational case, a large set of functions is defined by the equation. This explains why this kind of study is by no means sufficient in our case. Furthermore, it can be shown that, in the purely rational case ($q \geq 2$ as opposed to the integer case $q = 1$) with G and FIR filter, the requirement of the shift property $\varphi_s(t) = \varphi_0(t - s)$ in (28) would result in $\varphi_0(t) = 0$ as the only solution of the two-scale difference equation [3], [13]. The shift property cannot hold in the purely FIR rational case.

D. Support

Assume that the discrete schemes converge weakly to limit functions $\varphi_s(t)$. In a manner parallel to the dyadic case, these functions have a compact support. A rough estimate of this support is obtained by noting that, by construction, $g_j[n]$ cancels outside $[M_j \cdots L_j]$ where $L_j = L(p^j - q^j)/(p - q)$ and $M_j = M(p^j - q^j)/(p - q)$, while each $g_{j,s}[n]$ cancels outside $[M_j/q^j \cdots L_j/q^j]$. Since the resolution at iteration j is q^j/p^j, taking the limit when j tends to infinity leads to the following result:

$$\text{support } (\varphi_s) \subset \left[s + \frac{M}{p - q}, s + \frac{L}{p - q}\right]. \tag{32}$$

In fact, more accurate results can be obtained (see (74) in the Appendix) showing that the supports of each function are different. The differences between the supports of the functions φ_s are illustrated in Section IV-E. It turns out that, for the sets of functions which exhibit a smaller shift error, the difference between the length of these supports also becomes of less concern, since the values of the functions outside a common minimum interval, tend to vanish.

E. An Example: The Rational Equivalent of the Haar Function

This subsection is devoted to the study of the functions generated by the filter $G(z) = (1 - z^{-p})/(1 - z^{-1})$. The recurrence equations characterizing $\varphi_s(t)$ are

$$g_{0,s}[n] = \delta[n - s] \tag{33}$$

$$g_{j+1,s}[n] = \sum_k g[nq - kp]g_{j,s}[k] \tag{34}$$

$$= g_{j,s}[n_1] \tag{35}$$

where $n_1 = \lfloor nq/p \rfloor$. By induction, one can easily check that $g_{j,s}[n] = 1$ over an interval $[a_j[s], a_j[s + 1] - 1]$, and is zero elsewhere, where $a_j[s]$ are defined in the Appendix by (75), (76). Clearly, letting j tend to infinity leads to a set of functions $\varphi_s(t)$ indicator functions on the intervals

$$I_s = [\alpha[q - 1 + s(p - q)], \alpha[p - 1 + s(p - q)][\tag{36}$$

where $\alpha[s]$ is defined as in the Appendix by (77). These intervals are nonoverlapping and their union is the set of real numbers. The associated functions are the rational equivalent of the Haar low-pass functions in the dyadic case. For example in the case $p = 3$ and $q = 2$, we have $I_0 = [0, 1.622[$, $I_1 = [1.622, 2.433[$, $I_2 = [2.433, 3.65[$ and so on. It should be noted that the function $\varphi_{-1}(t)$ vanishes and that I_{-1} is empty. Of course these intervals have every different sizes, within the limit given in Section IV-D. This is a great difference with the classical integer case.

F. Properties

1) A Necessary Condition for Convergence: When do the iteration of rational schemes such as the one in Fig. 6 converge strongly? We prove that a necessary condition for this to be achieved is

$$\frac{z^{-p} - 1}{z^{-1} - 1} \text{ divides } G(z) \quad \text{and} \quad G(1) = p. \tag{37}$$

Proof: Let t be a real number and choose $C \geq \max(|M|, |L|, p(p - q))/(p - q)$. Then consider a sequence n_j such that $|n_j - t(p/q)^j| \leq C$ and such that $n_j \equiv \nu \pmod p$. Then $g_{j,s}[n_j]$ tends to $\varphi_s(t)$ when j tends to infinity by assumption. Since G is FIR, the sum in (25) has a finite number of terms; moreover it only involves integers k such that $|k - t(p/q)^j| \leq C$ due to the particular choice for C. So letting j increase we must have $\Sigma_k\, g[\nu q - kp] = 1$ for all ν between 0 and $p - 1$. This can also be written $\Sigma_k\, g[n - kp] = 1$ for all integer n and this is equivalent to (37). □

Note, that this relation shows a strong parallelism with the dyadic case where the corresponding condition is $(z + 1)$ divides $G(z)$ and $G(1) = 2$. In other words, the general rule is that the filter $G(z)$ should cancel at the aliasing frequencies $2\pi/p, 4\pi/p, \cdots, 2(p-1)\pi/p$ and should not vanish at frequency 0. This confirms its low-pass characteristic. This simple requirement is now shown to be closely related to the differentiability of the limit functions.

2) Derivative of the Limit Function: Suppose that the FIR filter $G(z)$ converges weakly to some limit functions $\varphi_s(t)$. We show below that, provided that $G^\bullet(z)$ is linked with $G(z)$ by the following relation:

$$G(z) = \frac{q}{p}\frac{z^{-p}-1}{z^{-q}-1}G^\bullet(z) \tag{38}$$

then the derivative of $\varphi_s(t)$ could be obtained as a simple combination of the limit functions associated to $G^\bullet(z)$

$$\varphi_s'(t) = \varphi_s^\bullet(t) - \varphi_{s+1}^\bullet(t). \tag{39}$$

Proof: Considering the function $\varphi_s(t)$ as a distribution, it is possible to differentiate it. If $\psi(t)$ is a C^∞ compactly supported function, we have $\int \varphi_s'\psi = -\int \varphi_s\psi'$. Thus,

$$\int \varphi_s'\psi = -\lim_{j\to\infty}\left(\frac{q}{p}\right)^j \sum_n g_{j,s}[n]\,\psi'\left(n\left(\frac{q}{p}\right)^j\right). \tag{40}$$

The fact that G is FIR shows that $\Sigma_n |g_{j,s}[n]| \le (p/q)^{\alpha j}$ for some integer α. We now carry out a Taylor expansion of the C^∞ function ψ until the order α around the point $n(q/p)^j$. It can be shown that the terms of order greater than 1 as well as the remainder of the expansion, do not contribute to the limit. This allows the change of $\psi'(t)$ by $(p/q)^j[\psi(t+(q/p)^j) - \psi(t)]$ in the sum, which results in

$$\int \varphi_s'\psi = \lim_{j\to\infty}\left(\frac{q}{p}\right)^j \sum_n w_{j,s}[n]\psi\left(n\left(\frac{q}{p}\right)^j\right) \tag{41}$$

with (42)

$$w_{j,s}[n] = \frac{g_{j,s}[n] - g_{j,s}[n-1]}{(q/p)^j}. \tag{43}$$

It is possible to check that $w_{j,s}[n]$ follows p/q-adic iterations as shown in Fig. 6, with $G^\bullet(z)$ as a low-pass filter. Since $g_{j,s}[n]$ converges, so do $w_{j,s}[n]$. By considering $j = 0$, it is easily seen that $w_{j,s}[n] = g_{j,s}^\bullet[n] - g_{j,s+1}^\bullet[n]$, which straightforwardly proves the weak convergence of the schemes based on $G^\bullet$ and leads to (39). □

For comparison purposes, we have in the dyadic case, $G(z) = (z^{-1}+1)G^\bullet(z)/2$ which is simply (38) for $p = 2$ and $q = 1$; we also have $\varphi'(t) = \varphi^\bullet(t) - \varphi^\bullet(t-1)$ which is merely (39) with the addition of the shift property. Interestingly, (39) shows that the regularity (either Hölder or Sobolev [20]) of the set of functions $\varphi_s(t)$ is *exactly* raised by 1 as compared to the regularity of the set of functions $\varphi_s^\bullet(t)$. Thus, the nonpolynomial factor $R(z) = (z^{-p}-1)/(z^{-q}-1)$ plays the role of a differentiation operator. This is to be compared to $1 + z^{-1}$ in the dyadic case.

It is not the purpose of this paper to answer all questions about the regularity of functions φ_s, since this will be done in another paper still in preparation [22]. However, one can say that in the rational case there exist two ways of building a more regular set of functions from an initial polynomial $G(z)$

- Either multiply the polynomial $G(z)$ by the fraction $R(z)$. This is possible only if $G(z)$ is divisible by $(z^{-q}-1)/(z^{-1}-1)$. In this case, the regularity is exactly raised by 1, and the generated functions are simply deduced from the initial ones with the help of (39).
- Or multiply the polynomial by $(z^{-p}-1)/(z^{-1}) - 1)$. This is always possible. In this case, the Hölder regularity exponent [20] is raised by more than 1 (but close to 1 anyway) [22]. However, the generated functions cannot easily be deduced from the initial ones.

3) Shift Error: As already shown in Section IV-E, FIR polynomials generate a set of functions without shift invariance. This shift error, although easy to see when plotting the functions, is much more difficult to estimate. A possible definition is the maximum error between any two limit functions brought back to the same interval

$$\epsilon = \sup_{s,s',t} |\varphi_s(t+s) - \varphi_{s'}(t+s')|. \tag{44}$$

Unfortunately, a fair estimate of this shift error, would require the computation of a number of functions which grows exponentially with the number of iterations. This is numerically intensive due to the low rate of convergence of each iterate to its limit function. The only practical result we could obtain in this direction is a lower bound; this is of course not very useful by nature. Because these estimates are unlikely to be very reliable, we are reluctant to give experimental values for the shift error of a given scheme. However, a major experimental result is that, provided that the generating polynomial contains enough factors of the type $(z^{-p}-1)/(z^{-1}-1)$, all the computed limit functions show a very small shift error; this error is even smaller than the accuracy of the estimation for the limit functions. This is not coincidental, and we recently obtained a theoretical estimate confirming this trend [22]; we shall however not make use of it in this paper. We develop these observations below.

An example illustrating the loss of shift property in rational schemes (here $p = 3$ and $q = 2$) is obtained for the following (nonnormalized) low-pass polynomial

$$G_1(z) = \left(\frac{z^{-3}-1}{z^{-1}-1}\right)^3 (2z^{-1}-1). \tag{45}$$

Ten limit curves with varying initialization polynomial z^{-s} are displayed in Fig. 9. A first remark is that the convergence is slower than in the dyadic case; the curves were obtained after 14 iterations, whereas the same precision would have been obtained after only eight iterations in the dyadic case. In fact, the difference between the limit functions and their jth iterates tends to zero as $(q/p)^j$—for sufficiently smooth functions—when j tends to infinity [22]. This explains why for a given precision $1/R$, we

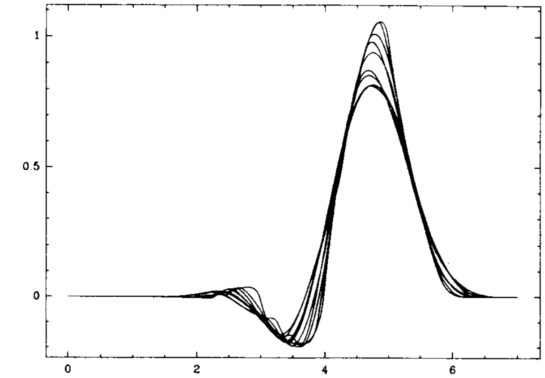

Fig. 9. $\varphi_s(t + s)$ for $s = 0 \cdots 9$ where $G(z) = (z^{-3} - 1/z^{-1} - 1)^3 (2z^{-1} - 1)$.

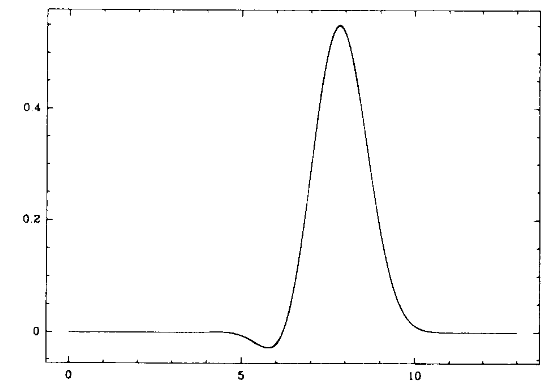

Fig. 10. $\varphi_s(t + s)$ for $s = 0 \cdots 9$ where $G(z) = (z^{-3} - 1/z^{-1} - 1)^6 (2z^{-1} - 1)$.

need approximately $j = \log(R)/\log(p/q)$ iterations in the rational case. This results stands for one function, but the computation of a maximum shift error between any two limit functions is another task. From (24) we can directly see that at iteration j, a set of q^j different function estimates has to be taken into account. It is generally impossible to compute all these functions. This would mean the computation of all the coefficients of the polynomial $G_j(z)$ that is to say $L(p^j - q^j)/(p - q)$ coefficients. This number is equivalent to

$$LR \frac{\log(p)}{\log(p/q)} \tag{46}$$

as R tends to infinity. In the example of Fig. 9 (14 iterations), a straightforward evaluation of (44) would need the computation of more than 3.3×10^7 coefficients $\cdots$

However, we have noticed that generating polynomials with a larger number of factors $(z^{-p} - 1)/(z^{-1} - 1)$ led to limit functions showing a dramatically decreased shift error. This is well depicted by Fig. 10 as compared to Fig. 9. The corresponding low-pass (non-normalized) polynomial is here

$$G_2(z) = \left(\frac{z^{-3} - 1}{z^{-1} - 1}\right)^3 G_1(z). \tag{47}$$

Once again, we have plotted only ten functions, but the other ones we computed showed the same behavior. The shift error between the ten iterates in this example was smaller (approximately 0.002) than the error between the iterates and their respective limit functions (approximately 0.003), which makes accurate experimental shift estimates difficult to obtain.

Since the required factors are closely related to the regularity of the limit functions (see Section IV-F), this suggests that more regular limit functions should show a smaller shift error.

V. Time-Frequency Transform Interpretation

The dyadic filter banks are not only simple tree architectures, allowing easy implementation for coding purposes, they also provide a discrete version of wavelet transforms, and a simple interpretation in terms of *multiresolution analysis* [16], [18]. This is changed in the p/q case due to the absence of shift property. However, we have seen in Section IV-F that constraining the polynomial $G(z)$ to include factors of the type $(z^{-p} - 1)/(z^{-1} - 1)$ increases the regularity and decreases the shift error between the various limit functions. Taking this fact into account, we outline here that the same properties can be found in the p/q-adic iterated filter banks as in the dyadic case, up to an "error" which can be made arbitrarily small by an *ad hoc* choice of the generating polynomial.

This is undertaken by interpreting the outputs of the filter bank depicted in Fig. 7 in terms of the limit functions generated by iterating the synthesis part of Fig. 8. Since this interpretation involves some time-reversal of the limit functions, we use a compact notation for this: given an arbitrary set $f_s(t)$ of functions, we build a new time-reversed set f_s^- which we define by $f_s^-(t) = f_{-s}(-t)$. Otherwise, from now on, the notations for the output of the iterated analysis filter bank are given in Fig. 1.

A. A Wavelet Transform?

Assume now, that one can find an analog signal $x(t)$ such that the input $x_0[n]$ of the iterated analysis rational two-band filter bank can be considered as its nth weighted sample as follows $x_0[n] = \int x(t)\varphi_n^-(t)\,dt$. Then, an easy induction [taking advantage of the two-scale equation (28)] proves that the outputs of the analysis scheme of Fig. 7 are provided by

$$x_j[n] = \int x(t)\varphi_n^-\left(\left(\frac{p}{q}\right)^{-j} t\right) dt \tag{48}$$

$$y_j[n] = \int x(t)\psi_n^-\left(\left(\frac{p}{q}\right)^{-j} t\right) dt \tag{49}$$

where $\psi_n^-(t)$ are the time-reversed of the "mother" functions $\psi_n(t)$ (terminology of [18])

$$\psi_n(t) = \sum_k h[k(p - q) - np]\varphi_k\left(\frac{p}{q}t\right). \tag{50}$$

These formulas are the exact equivalent of the discrete wavelet transform in the dyadic case. We obtain a discrete wavelet transform for the low-pass iteration if we formally substitute $\varphi(t-n)$ for $\varphi_n(t)$ in (48). In the same way, for the high-pass iteration (49) a shift error is associated with the functions $\psi_s(t)$. More precisely we can define

$$\eta = \sup_{s,s',t} \left| \psi_s\left(t + s\frac{q}{p-q}\right) - \psi_{s'}\left(t + s'\frac{q}{p-q}\right) \right|. \quad (51)$$

In cases that we are studying later, this error can be minimized. This suggests that it is possible to compute a discrete wavelet transform $\mathrm{DWT}_{j,n}[x]$ of signal $x(t)$ for the scale parameters $(p/q)^{-j}$ and the discretized time unit $(p/q)^j q/(p-q)$

$$\mathrm{DWT}_{j,n}[x] = \int x(t)\psi_0^-\left(\left(\frac{p}{q}\right)^{-j} t - n\frac{q}{p-q}\right) dt \quad (52)$$

by means of schemes as depicted in Fig. 7.

1) Loss of the Shift Property for the High-Pass Functions: The natural shift unit of the limit function $\varphi_s(t)$ is 1 since the supports of these functions are shifted between themselves by the same amount (see Section IV-D). This is not the case for the high-pass functions ψ_s whose natural shift unit is $q/(p-q)$. This is a consequence of (32) from which the support of the functions ψ_s can be obtained. This justifies the definition of the high-pass shift error (51). With this modification, does $\psi_s(t) = \psi_0(t - sq/(p-q))$ strictly hold in the case where the low- and high-pass filters are FIR? This would ensure that the outputs $y_j[n]$ of the filter banks be equal to $\mathrm{DWT}_{j,n}[x]$. This is unfortunately not possible, at least in the most interesting case when the convergence of the rational schemes is strong (the proof, too long, will be given in [22]). We must thus evaluate the shift error (51); the outputs $y_j[n]$ can be then made as close as desired to $\mathrm{DWT}_{j,n}[x]$ if it is possible to minimize this shift error.

2) Shift Error: The shift error of the functions $\psi_s(t)$ can be estimated in connection with the shift error of the functions $\varphi_s(t)$. With respect to this problem, there is an important difference between the cases $p-q=1$ and $p-q\neq 1$.

- If $p-q=1$, (49) shows that $|\psi_s(t+sq) - \psi_{s'}(t+s'q)| \leq \epsilon \sum_k |h[k]|$, according to the definition of the shift error ϵ given in Section IV-F. Thus, decreasing the low-pass shift error also decreases the high-pass shift error.
- if $p-q\neq 1$, define $p-q$ new functions $a_{s_0}(t)$ for $s_0 = 0 \cdots (p-q-1)$ as follows:

$$a_{s_0}\left(t - s_0\frac{q}{p-q}\right) = \sum_k h[k(p-q) - s_0 p]\varphi_0\left(\frac{p}{q}t - k\right). \quad (53)$$

Then, one can characterize a shift error among subsets of the functions ψ_s. Namely, for each s_0 and $s \equiv s_0 \pmod{p-q}$

$$\left|\psi_s(t) - a_{s_0}\left(t - s\frac{q}{p-q}\right)\right| \leq \epsilon \sum_k |h[k(p-q) - s_0 p]|. \quad (54)$$

This shows that inside each subset of functions whose indexes are congruent modulo $p-q$, the shift error is also directly related to the low-pass shift error. However, the shift error between *different* subsets depends not only on the low-pass filter, but also on the high-pass one, as is clearly seen from (53). Even if the shift error were canceled for the low-pass functions φ_s, this would not be the case in general for the high-pass functions ψ_s, but possibly for an adequate choice of $H(z)$. However, we have not yet investigated the issue of how $H(z)$ should be chosen in order to make this shift error between subsets as small as possible. We were mostly interested in the case $p-q=1$ because of its finer frequency resolution.

B. Biorthonormality and Perfect Reconstruction

For any couple $f, g \in L^2$, define the L^2 scalar product by

$$\langle f, g\rangle = \int f(t)g(t)\,dt. \quad (55)$$

With respect to this scalar product, the functions $\varphi_s(t)$ do not in general represent an orthonormal set, that is to say $\langle \varphi_s, \varphi_{s'}\rangle \neq \delta[s-s']$. However, the synthesis filters $p/q\check{G}(z)$ and $p/q\check{H}(z)$ generate functions $\check{\varphi}_n$ and $\check{\psi}_n$ which are biorthonormal to the analysis functions, as shown below. Since we work under critical sampling involving a square polyphase matrix as stated in part 1, one can swap both matrices in (12) and get $\Gamma\check{\Gamma} = \mathrm{Id}$, which leads to

$$\delta[n-n'] = \sum_k g[np-kq]\check{g}[kq-n'p] \quad (56)$$

$$\delta[n-n'] = \sum_k h[np-k(p-q)]\check{h}[k(p-q)-n'p] \quad (57)$$

$$0 = \sum_k g[np-kq]\check{h}[k(p-q)-n'p] \quad (58)$$

$$0 = \sum_k h[np-k(p-q)]\check{g}[kq-n'p]. \quad (59)$$

Equation (56) can be iterated in order to involve $g_j[n]$ and $\check{g}_j[n]$, and if we assume the strong convergence for both sets of functions, we get $\delta[n-n'] = \langle \varphi_n^-, \check{\varphi}_{n'}\rangle$. The system of equations (56)–(59) can finally be seen as equivalent to the following biorthonormality constraints:

$$\delta[n-n'] = \langle \varphi_n^-, \check{\varphi}_{n'}\rangle \quad (60)$$

$$\delta[n-n'] = \langle \psi_n^-, \check{\psi}_{n'}\rangle \quad (61)$$

$$0 = \langle \varphi_n^-, \check{\psi}_{n'}\rangle \quad (62)$$

$$0 = \langle \psi_n^-, \check{\varphi}_{n'}\rangle \quad (63)$$

which is true for every couple of integers n, n'. This remarkable result is the same one as previously obtained in the dyadic case. The analysis and synthesis functions form a biorthonormal set, when perfect reconstruction is achievable. An immediate consequence of the equation is that (61) can be extended to

$$\int \psi_n^- \left(\frac{p^j}{q^j} t\right) \check{\psi}_{n'} \left(\frac{p^{j'}}{q^{j'}} t\right) dt = \frac{p^j}{q^j} \delta[n - n']\delta[j - j'] \tag{64}$$

which can be described as interscale biorthonormality.

Note that, in the p/q case, *biorthogonality* (defined by $\langle \varphi_n, \check{\varphi}_{n'} \rangle = C(n)\delta[n - n']$ with $C \neq 0$) is somewhat different from *biorthonormality* (which requires $C = 1$). Unlike the dyadic case, biorthonormality is a stronger property than biorthogonality, since the scalar product $\langle \varphi_n, \check{\varphi}_{n'} \rangle$ does not equate $\langle \varphi_{n-n'}, \check{\varphi}_0 \rangle$. This makes biorthogonality more difficult to approach, but it may be fruitful to progress in this direction. A simple example of the orthogonal set (biorthogonal, with the same analysis and synthesis functions) is the "generalized Haar" scheme exhibited in Section IV-E, but we are not studying biorthogonality further is this paper.

1) Pseudo-Wavelet Series: Reconstruction can then be seen from another point of view. Given a sequence $x_0[n]$, we build the analog signals

$$x_j(t) = \sum_n \frac{q^j}{p^j} x_j[n]\check{\varphi}_n \left(\frac{q^j}{p^j} t\right) \tag{65}$$

$$y_j(t) = \sum_n \frac{q^j}{p^j} y_j[n]\check{\psi}_n \left(\frac{q^j}{p^j} t\right) \tag{66}$$

where $x_j[n]$, $y_j[n]$ are still the low-pass and high-pass outputs of the analysis filter bank (Fig. 7) after j iterations. Thus, $y_j(t)$ contains the information of $x_0[n]$ at scale j, while $x_j(t)$ contains the information at scales j and higher. Due to biorthonormality [and in particular (64)], we have the reconstruction relation

$$x_0(t) = x_N(t) + \sum_{j=1}^{N} y_j(t) \tag{67}$$

which provides a development of the input signal into a "pseudo-wavelet" series plus a remainder (the low-pass term, $x_N(t)$ of the series). Formula (67) is in fact the analog equivalent of the discrete reconstruction procedure based on iterating the synthesis rational filter bank (Fig. 7). This presentation makes a natural introduction to a "multiresolution" point of view of the rational filter bank schemes.

C. Multiresolution Analysis

Still in the two-channel case, we extend the definition of multiresolution analysis (better known in the dyadic case [16]-[18]) to the rational case. We define the spaces

$$V_n^- = \overline{\text{span}\left\{\varphi_s^- \left(\left(\frac{p}{q}\right)^n t\right)\right\}_{s\in Z}} \cap L^2. \tag{68}$$

Due to the time reverse definition of φ_s^-, these functions obey a two-scale equation (28) based on $G(z^{-1})$, hence the spaces V_n^- are embedded

$$\cdots \subset V_{-1}^- \subset V_0^- \subset V_1^- \subset \cdots L^2. \tag{69}$$

One can observe that the spaces V_n^- include higher resolution functions as n increases. Defining the spaces

$$W_n^- = \overline{\text{span}\left\{\psi_s^- \left(\left(\frac{p}{q}\right)^n t\right)\right\}_{s\in Z}} \cap L^2 \tag{70}$$

it is clear from (50) that $W_n^- \subset V_{n+1}^-$. The perfect reconstruction relation is thus equivalent to the direct sum equation on the sets

$$W_n^- \oplus V_n^- = V_{n+1}^-. \tag{71}$$

By induction, this equation means that the larger space V_0^- can be decomposed into a direct sum of given decreasing resolution spaces W_n^- plus the smaller space V_{-N}^-, containing lower resolution functions

$$V_0^- = W_{-1}^- \oplus W_{-2}^- \oplus \cdots \oplus W_{-N}^- \oplus V_{-N}^-. \tag{72}$$

This last equation is equivalent to (67). Under conditions we have not yet investigated (for the dyadic case see [4]), if the decomposition is continued to infinity, it should be possible to develop any square integrable function into a "pseudo-wavelet" series. In any case, this decomposition of L^2 is not always true. A simple example is readily obtained with the filter $G(z) = p/q(z^{-q} - 1)/(z^{-1} - 1)$. The limit functions are dirac impulses directly linked to the derivative of the generalized Haar functions (Section IV-E). These functions are not in L^2, thus $V_j = 0$ for all j and finally, their union fails to give L^2.

A dual multiresolution analysis $\check{V}_n$ and $\check{W}_n$ is associated to the synthesis functions $\check{\psi}_s$ and $\check{\psi}_s$. Interscale biorthonormality (64) leads to

$$W_n^- \perp \check{W}_{n'}^- \qquad \text{for all } n \neq n'. \tag{73}$$

Both analyses are in general distinct, but an important particular case arises when they are not. This leads to orthonormal functions obeying a two-scale equation. The functions are the same ones at the synthesis and analysis sides, and the pseudo-wavelet series (67) is an orthonormal development.

VI. Conclusion

This paper focused on the properties of iterated two-band rational filter banks. We showed that, despite the strong parallelism between the dyadic and the rational case, many differences between both situations were due to the absence of shift property.

The first apparent difference was that there is no more a single limit function characterizing the infinite iteration of such schemes. There is instead an infinity of them. However, many properties are simple extensions of the dyadic case, such as derivation and compact support.

The loss of shift property also forbids the high-pass outputs to strictly behave like sampled wavelet transforms in the case of FIR analysing filters. However, the situation is not as dark as it seems at first sight. A suitable choice for the filters can actually reduce the "shift error" between the various limit functions generated by the low-pass filter. Furthermore, the shift error between the associated high-pass functions in the most interesting case $p - q = 1$ also decrease accordingly, so that we can "almost" obtain a wavelet transform.

The important point is that, wherever we can accommodate for a small error, we can work with rational filter banks in the same way as with dyadic filter banks, with the advantage of a finer frequency resolution. A future work under writing [22] proves most results that are only illustrated in the present paper, concerning mainly the links between regularity and shift error. However, much remains to be done on iterated rational filter banks, beginning with the study of orthonormal functions, or filter design.

The precise characterization of rational filter banks outlined in this paper might be helpful, especially in order to analyze or code efficiently speech or audio signals (which require a more precise analysis than the classical octave band analysis). We expect in particular the shift error to be an important parameter for the design of such filter banks, together with more classical frequency domain ones like transition band, or attenuation.

Appendix
Support—More Accurate Values

A closer examination of the degree of $z^{-s}G_{j,s}(z)$ shows that

$$\text{support } (\varphi_s) \subset [\alpha[q - 1 + M + s(p - q)], \alpha[L + s(p - q)]] \quad (74)$$

where the real sequence $\alpha[s]$ is defined as follows: fixing the integer s, consider the integer sequence $\alpha_j[s]$ defined by recursion over j by

$$\alpha_0[s] = 0 \quad (75)$$

$$\alpha_{j+1}[s] = \left\lfloor \frac{s + p\alpha_j[s]}{q} \right\rfloor \quad (76)$$

then

$$\alpha[s] = \lim_{j \to \infty} \left(\frac{p}{q}\right)^{-j} \alpha_j[s]. \quad (77)$$

Proof: Assume that $g_{j,s}[n]$ converges (weakly is sufficient) toward $\varphi_s(t)$. In fact, there exists two sequences $a_j[s] \le b_j[s]$ such that $g_{j,s}[n] = 0$ for all n outside the interval $[a_j, b_j]$. From (25), it appears that

$$\frac{M}{q} + \frac{p}{q} a_j[s] \le \frac{a_{j+1}[s]}{b_{j+1}[s]} \le \frac{L}{q} + \frac{p}{q} b_j[s] \quad (78)$$

and the sequences thus satisfy the following recursions:

$$\begin{cases} a_0[s] = s \\ a_{j+1}[s] = \left\lfloor \dfrac{q - 1 + M + pa_j[s]}{q} \right\rfloor \end{cases}$$

and

$$\begin{cases} b_0[s] = s \\ b_{j+1}[s] = \left\lfloor \dfrac{L + pb_j[s]}{q} \right\rfloor. \end{cases} \quad (79)$$

Of course, if it happens that $a_j[s]$ becomes greater than $b_j[s]$ then $g_{j,s}[n]$ vanishes (can only happen if $L < q - 1$). Equations (75) and (76) show that

$$a_j[s] = s + \alpha_j[q - 1 + M + s(p - q)] \quad (80)$$

$$b_j[s] = s + \alpha_j[L + s(p - q)]. \quad (81)$$

This indicates that it is sufficient to study the sequence α_j. We need to know if $(q/p)^j\alpha_j[s]$ converges towards a finite value. In fact, if $r_j[s]$ is the remainder of the Euclidean division of $s + p\alpha_j[s]$ by q, it can be seen that it is the case and that the convergence is geometric

$$\alpha[s] = \lim_{j \to \infty} \left(\frac{p}{q}\right)^{-j} \alpha_j[s] = \frac{s}{p - q} - \sum_{j \ge 0} r_j[s] \frac{q^j}{p^{j+1}}. \quad (82)$$

Moreover, since $r_j[s]$ lies between 0 and $q - 1$, we have the inequality

$$\frac{s - q + 1}{p - q} \le \alpha[s] \le \frac{s}{p - q}. \quad (83)$$

That is to say, the functions (or distributions) $\varphi_s(t)$ have compact support

$$[\alpha[q - 1 + M + s(p - q)], \alpha[L + s(p - q)]] \quad (84)$$

□

The lower bound of the interval lies between $s + M/(p - q)$ and $s + (M + q - 1)/(p - q)$, whereas the upper bound lies between $s + (L - q + 1)/(p - q)$ and $s + L/(p - q)$. This is the reason why, for the sake of simplicity we say that $\varphi_s(t)$ is supported by the interval $[s + M/(p - q), s + L/(p - q)]$. However, the support is strictly included in this interval. Note, finally, that in the integer case ($q = 1$) our result reduces to the classical one [8].

Acknowledgment

The author is much indebted to P. Duhamel for spending much of his time reading the manuscript and proposing numerous changes which greatly improve the writing of the paper. Thanks also are due to O. Rioul for fruitful discussions and for first introducing the author to the works of J. Kovačević and M. Vetterli, as well as to the reviewers for their constructive remarks.

References

[1] P. Auscher, "Ondelettes fractales et applications," Ph.D. dissertation, Univ. Paris, Paris, France, 1989.
[2] G. Bi, "Minimization of delay requirements for rational sampling rate alternating systems," in *Proc. ICASSP*, Toronto, Ont., Canada, May 1991, vol. 3, pp. 1817-1820.
[3] A. Cohen and I. Daubechies, "Orthonormal bases of compactly sup-

ported wavelets III. Better frequency resolution,'' *Siam J. Math. Anal.*, vol. 24, pp. 520-527, Mar. 1993.

[4] A. Cohen, I. Daubechies, and J. C. Feauveau, ''Biorthogonal basis of compactly supported wavelets,'' *Commun. Pure Appl. Math.*, vol. 45, pp. 485-560, 1992.

[5] R. E. Crochiere and L. R. Rabiner, ''Interpolation and decimation of digital signals—A tutorial review,'' *Proc. IEEE*, vol. 69, pp. 300-331, Mar. 1981.

[6] A. Croisier, D. Esteban, and C. Galand, ''Perfect channel splitting by use of interpolation/decimation/tree decomposition techniques,'' in *Proc. Int. Conf. Inform. Sci. Syst.*, Patras, Greece, Aug. 1976, pp. 443-446.

[7] I. Daubechies, ''Orthonormal bases of compactly supported wavelets,'' *Commun. Pure Appl. Math.*, vol. 41, pp. 909-996, Nov. 1988.

[8] I. Daubechies and J. Lagarias, ''Two-scale difference equations I. Existence and global regularity of solutions,'' *Siam J. Math. Anal.*, vol. 22, pp. 1388-1410, Sept. 1991.

[9] P. Goupillaud, A. Grossmann, and J. Morlet, ''Cycle-octave and related transforms in seismic signal analysis,'' *Geoexploration*, vol. 23, pp. 85-102, Elsevier, Amsterdam, The Netherlands, 1984/1985.

[10] M. Holschneider, R. Kronland-Martinet, J. Morlet, and Ph. Tchamitchian, ''A real-time algorithm for signal analysis with the help of the wavelet transform,'' in *Wavelets, Time-Frequency Methods and Phase Space*, J. M. Combes, *et al.* Eds. New York: Springer 1989, pp. 286-297.

[11] C.-C. Hsiao, ''Polyphase filter matrix for rational sampling rate conversions,'' in *Proc. ICASSP*, Dallas, TX, Apr. 1987, pp. 2173-2176.

[12] S. Kadambe and G. F. Boudreaux-Bartels, ''A comparison of wavelet functions for pitch detection of speech signals,'' in *Proc. ICASSP*, Toronto, Ont., Canada, May 1991, pp. 449-452.

[13] J. Kovačević, ''Filter banks and wavelets: Extensions and applications,'' Ph.D. dissertation, Columbia Univ., New York, NY, 1991.

[14] J. Kovačević and M. Vetterli, ''Perfect reconstruction filter banks with rational sampling rate changes,'' in *Proc. ICASSP*, Toronto, Ont., Canada, May 1991, vol. 3, pp. 1785-1788.

[15] ——, ''Perfect reconstruction filter banks with rational sampling rate changes in one and two dimensions,'' in *Proc. SPIE Conf. Visual Commun. Image Processing*, Philadelphia, PA, Nov. 1989, pp. 1258-1268.

[16] S. Mallat, ''A theory for multiresolution signal decomposition: The wavelet decomposition,'' *IEEE Trans. Patt. Anal. Mach. Intell.*, vol. 11, pp. 674-693, July 1989.

[17] ——, ''Multifrequency channel decompositions of images and wavelet models,'' *IEEE Trans. Acoust., Speech, Signal Processing*, vol. 37, pp. 2091-2110, Dec. 1989.

[18] Y. Meyer, *Ondelettes*. Paris: Hermann, 1990.

[19] K. Nayebi, T. P. Barnwell III, and M. J. T. Smith, ''The design of perfect reconstruction nonuniform band filter banks,'' in *Proc. ICASSP*, Toronto, Ont., Canada, May 1991, vol. 3, pp. 1781-1784.

[20] O. Rioul, ''Simple regularity criteria for subdivision schemes,'' *Siam. J. Math. Anal.*, vol. 23, pp. 1544-1576, Nov. 1992.

[21] O. Rioul and P. Duhamel, ''Fast algorithm for discrete and continuous wavelet transforms,'' *IEEE Trans. Inform. Theory*, vol. 38, pp. 569-586, Mar. 1992.

[22] O. Rioul and T. Blu, ''Simple regularity criteria for subdivision schemes. II. The rational case,'' in preparation.

[23] R. W. Schafer and L. R. Rabiner, ''A digital signal processing approach to interpolation,'' *Proc. IEEE*, vol. 61, pp. 692-702, June 1973.

[24] M. J. Shensa, ''Affine wavelets: Wedding the ''à trous'' and Mallat algorithms,'' *IEEE Trans. Signal Processing*, vol. 40, pp. 2464-2482, Oct. 1992.

[25] P. P. Vaidyanathan, ''Quadrature mirror filter banks, *M*-band extensions and perfect-reconstruction techniques,'' *IEEE ASSP Mag.*, vol. 4, pp. 4-20, July 1987.

[26] ——, ''Multirate digital filters,'' filter banks, polyphase networks and applications: A tutorial, *Proc. IEEE*, vol. 78, pp. 56-93, Jan. 1990.

[27] M. Vetterli, ''A theory of multirate filter banks,'' *IEEE Trans. Acoust., Speech, Signal Processing*, vol. ASSP-35, pp. 356-372, May 1987.

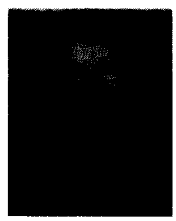

Thierry Blu was born in Orléans, France, in 1964. He graduated from École Polytechnique, France, in 1986, and from Télécom Paris, Paris, France, in 1988.

He is currently with France Télécom-CNET (National Center for Telecom Studies), Issy-les-Moulineaux, France. His research interests include digital signal processing, multirate filter banks, and wavelet transforms.